CHAPTER 83

Nonlinear Wave Transformation Over a Submerged Permeable Breakwater

Eric C. Cruz[1], Masahiko Isobe[2] and Akira Watanabe[2]

Abstract

A set of nonlinear vertically integrated equations has been derived to predict the transformation of waves over a submerged permeable breakwater on a one-dimensional topography. The square of the relative water depth is assumed to be of the same order as the wave height to water depth ratio and a set of second-order governing equations which are equivalent to the Boussinesq equations is derived. The equations have been applied to simulate non-breaking and breaking wave transformations obtained from laboratory experiments, in the latter incorporating a model for breaking wave energy dissipation. When breaking is nonexistent on the breakwater, the wave height as well as the wave profile is well predicted. However, the disintegrating character of the transmitted waves is weakly predicted. For breaking transformation, the wave profiles are predicted well prior to the lee of the breakwater where disintegration occurs.

1 Introduction

In recent years, submerged permeable breakwaters have been constructed in coastal zones to provide protection against wave attack. This type of breakwater has become popular mainly because of its advantages on aesthetic and environmental considerations. Submergence below the water surface and the porosity of the breakwater cause part of the incident wave energy to pass through the structure. Although the structure allows a level of wave transmission into the protected zone, it dissipates wave energy considerable enough to protect a beach from erosion by generating turbulence in the porous medium and causing the waves to break over the structure.

[1]Graduate Student, Department of Civil Engineering, University of Tokyo, Hongo 7–3–1, Bunkyo-ku, Tokyo 113, Japan

[2]Professor, Department of Civil Engineering, University of Tokyo, ditto

A model describing wave transformation is an indispensable tool in coastal planning and design. For submerged permeable breakwaters, mathematical models have been developed so far on the basis of the linear sinusoidal wave theory (Rojanakamthorn et. al., 1980). However, since the nonlinearity of waves cannot be neglected on the breakwater, the models must be improved to predict the transformation accurately.

In this paper, a model of wave transformation that considers the nonlinearity of the waves, arbitrary bathymetry of the bed and nonlinear wave damping due to the porosity of the submerged breakwater is presented. Since the model equations are unsteady, they can be applied to irregular waves with suitable boundary conditions.

2 Basic Equations and Boundary Conditions

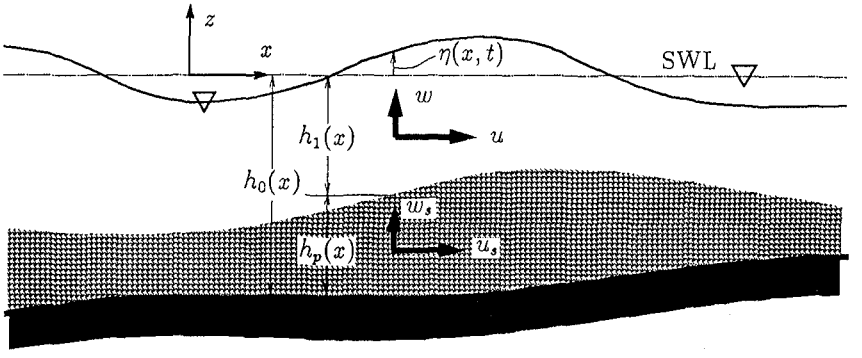

Figure 1: Definition of variables

The region of interest is shown in Figure 1. The depth of the free water layer is $h_1(x)$ and that of the porous layer is $h_p(x) = h_0(x) - h_1(x)$. The horizontal and vertical components of fluid particle velocity and pressure are u, w, p in the water layer and u_s, w_s, p_s in the porous layer. The subscript s refers to seepage quantities representing the flow within the pores only. The water surface displacement due to wave motion is $\eta(x,t)$. The fluid in the water layer is assumed inviscid and Euler's equation of motion in two dimensions are used:

$$\frac{\partial u}{\partial t} + u\frac{\partial u}{\partial x} + w\frac{\partial u}{\partial z} = -\frac{1}{\rho}\frac{\partial p}{\partial x} \qquad (-h_1 \le z \le \eta) \tag{1}$$

$$\frac{\partial w}{\partial t} + u\frac{\partial w}{\partial x} + w\frac{\partial w}{\partial z} = -g - \frac{1}{\rho}\frac{\partial p}{\partial z} \qquad (-h_1 \le z \le \eta) \tag{2}$$

where ρ is the mass density of water and g the gravitational acceleration.

The flow within the porous layer is governed by Euler's equation if proper account is taken for the effect of the divergence and convergence of streamlines caused by the presence of solid particles and for the loss of momentum caused by laminar flow along the granular surfaces and momentum loss through turbulence within the pores. The first effect is that of the virtual mass and the second is that of friction between the fluid and the grains. For steady flow in large granular medium, the drop in piezometric head results from laminar viscous resistance for low-velocity flow and a turbulent friction resistance for the high-velocity regime:

$$-\frac{1}{\rho}\nabla(p_s+\gamma z)=\frac{\nu}{K_p}\epsilon\vec{u}_s+\frac{C_f}{\sqrt{K_p}}\epsilon^2|\vec{u}_s|\vec{u}_s \tag{3}$$

where $\vec{u}_s=(u_s,w_s),\nabla=(\partial/\partial x,\partial/\partial z),\gamma$ the unit weight of water, ν the kinematic viscosity of water, K_p the intrinsic permeability, C_f a turbulent friction coefficient and ϵ the porosity. The constant K_p (dimension: length^2) and the coefficient C_f are determined from laboratory tests under standard conditions. The investigations of Shuto and Hashimoto (1970) showed that the resistance characteristics of steady and oscillatory flows do not significantly differ so that Eq.(3) can be applied to wave motion, which is under consideration here. The equations of unsteady motion for the porous layer $(-h_o\le z\le -h_1)$ therefore become

$$C_r\left(\frac{\partial u_s}{\partial t}+u_s\frac{\partial u_s}{\partial x}+w_s\frac{\partial u_s}{\partial z}\right)=-\frac{1}{\rho}\frac{\partial p_s}{\partial x}-\frac{\epsilon\nu}{K_p}u_s-\frac{\epsilon^2C_f}{\sqrt{K_p}}u_s\sqrt{u_s^2+w_s^2} \tag{4}$$

$$C_r\left(\frac{\partial w_s}{\partial t}+u_s\frac{\partial w_s}{\partial x}+w_s\frac{\partial w_s}{\partial z}\right)=-g-\frac{1}{\rho}\frac{\partial p_s}{\partial z}-\frac{\epsilon\nu}{K_p}w_s-\frac{\epsilon^2C_f}{\sqrt{K_p}}w_s\sqrt{u_s^2+w_s^2} \tag{5}$$

The effect of the virtual mass is expressed by the inertial coefficient $C_r=1+(1/\epsilon-1)C_M$, where C_M is the added mass coefficient.

For the incompressible fluid assumed here, the divergence of the velocity vector, as required by continuity, must vanish:

$$\frac{\partial u}{\partial x}+\frac{\partial w}{\partial z}=0 \qquad (-h_1\le z\le\eta) \tag{6}$$

$$\frac{\partial u_s}{\partial x}+\frac{\partial w_s}{\partial z}=0 \qquad (-h_o\le z\le -h_1) \tag{7}$$

The passage of a wave creates oscillatory motion in the two layers. This motion is subjected to the following boundary conditions:

- At the free surface, the usual dynamic and kinematic boundary conditions are enforced:

$$p=0 \qquad (z=\eta) \tag{8}$$

$$\frac{\partial\eta}{\partial t}+u\frac{\partial\eta}{\partial x}=w \qquad (z=\eta) \tag{9}$$

- At the bottom of the porous layer, the usual kinematic condition is applied:

$$w_s + u_s \frac{\partial h_0}{\partial x} = 0 \qquad (z = -h_o) \tag{10}$$

- The pressure and mass flux must be continuous at the water layer–porous layer interface, that is,

  interface continuity of pressure:

$$p = p_s \qquad (z = -h_1) \tag{11}$$

  interface continuity of mass flux:

$$w + u\frac{\partial h_1}{\partial x} = \epsilon \left(w_s + u_s \frac{\partial h_1}{\partial x} \right) \qquad (z = -h_1) \tag{12}$$

Equations (1), (2), (4) to (7) govern the unsteady, incompressible fluid motion in the water and porous layers subject to the boundary conditions Eqs.(8) to (12).

3 Nonlinear Equations for One-dimensional Wave Transformation on a Porous Bed

3.1 Assumption

In theory, the governing equations together with the boundary conditions can be solved for the primitive variables u, w, u_s, w_s, p and p_s. Since both sets of equations are highly nonlinear and involve η which is not known *a priori*, this undertaking is a tremendous, if not an impossible, task. In order to reduce the number of unknowns in these equations, a vertical integration of the governing equations is performed considering the nonlinear nature of the terms.

Let l be a characteristic length of the wave motion and h a characteristic depth giving a characteristic velocity $\sqrt{gh}$. Dimensional coordinates are nondimensionalized by l and h, velocities by $\sqrt{gh}$, pressures by ρgh and time by $l/\sqrt{gh}$ giving the nondimensional (primed) quantities:

$$x' = x/l \qquad z' = z/h \qquad t' = t/(l/\sqrt{gh}) \tag{13}$$

$$u' = u/\sqrt{gh} \quad w' = w(l/h)/\sqrt{gh} \quad u'_s = u_s/\sqrt{gh} \quad w'_s = w_s(l/h)/\sqrt{gh} \tag{14}$$

$$p' = p/\rho gh \qquad p'_s = p_s/\rho gh \tag{15}$$

Applying Eqs.(13) to (15) in the momentum equations, the following nondimensionalized equations of motion along z are obtained:

From equation (2),

$$\rightarrow \left(\frac{h}{l}\right)^2 \left(\frac{\partial w'}{\partial t'} + u'\frac{\partial w'}{\partial x'} + w'\frac{\partial w'}{\partial z'}\right) = -1 - \frac{\partial p'}{\partial z'} \tag{16}$$

From equation (5),

$$\rightarrow \left(\frac{h}{l}\right)^2 C_r \left(\frac{\partial w_s'}{\partial t'} + u_s'\frac{\partial w_s'}{\partial x'} + w_s'\frac{\partial w_s'}{\partial z'}\right) =$$

$$-1 - \frac{\partial p_s'}{\partial z'} - \left(\frac{h}{l}\right)^2 \frac{\epsilon\nu l}{K_p\sqrt{gh}} w_s' - \left(\frac{h}{l}\right)^2 \frac{\epsilon^2 C_f l}{\sqrt{K_p}} w_s' \sqrt{u_s'^2 + (h/l)^2 w_s'^2} \tag{17}$$

To describe waves in shallow water, the dispersion and nonlinearity should be taken into account. As in the case of the Boussinesq equations, the following assumption is made:

$$u' \sim w' \sim u_s' \sim w_s' \sim w_s' \sim O(\varepsilon) \sim (h/l)^2 \sim \delta^2 \tag{18}$$

3.2 First-order Approximation

To get a first-order formulation of the governing equations, terms of order ε^2 and higher in the nondimensional equations of motion are dropped from the corresponding dimensional counterparts invoking the assumption Eq.(18). Hence Eq.(16) gives the dimensional equation

$$0 = -g - \frac{1}{\rho}\frac{\partial p}{\partial z} \tag{19}$$

Integrating from $z = \eta$ to $z = z$ and applying the dynamic free surface condition, the last equation becomes

$$p = \rho g(\eta - z) \tag{20}$$

Similarly, integrating the first-order form of Eq.(5) and invoking the interface continuity of pressure and Eq.(24) give

$$p_s = \rho g(\eta - z) \tag{21}$$

The first-order form of Eq.(1) reduces to

$$\frac{\partial u}{\partial t} = -\frac{1}{\rho}\frac{\partial p}{\partial x}$$

and, invoking Eq.(20), becomes

$$\frac{\partial u}{\partial t} = -g\frac{\partial \eta}{\partial x} \tag{22}$$

Similarly, Eq.(4) reduces to

$$C_r \frac{\partial u_s}{\partial t} = -\frac{1}{\rho}\frac{\partial p_s}{\partial x} - \frac{\epsilon\nu}{K_p} u_s$$

and, using Eq.(21), gives

$$C_r \frac{\partial u_s}{\partial t} = -g\frac{\partial \eta}{\partial x} - \frac{\epsilon\nu}{K_p} u_s \tag{23}$$

From Eqs.(22) and (23), u and u_s do not depend on z (at least in the first order).

The kinematic boundary conditions are utilized after the continuity equations have been integrated. In the integration, Liebnitz rule is applied:

Integrating Eq.(7) from $z = -h_0$ to $z = z$, the following is obtained:

$$0 = \frac{\partial}{\partial x}\int_{-h_o(x)}^{z} u_s dz + w_s|_z - \frac{\partial h_o}{\partial x} u_s|_{-h_o} - w_s|_{-h_o}$$

From the bottom boundary condition Eq.(10), the last two terms in the right-hand side vanish, giving

$$w_s(z) = -\frac{\partial}{\partial x}[u_s(z + h_o)] \tag{24}$$

Similarly, Eq.(7) is integrated from $-h_o$ to $-h_1$ and the bottom kinematic boundary condition is invoked, giving

$$w_{s,-h_1} + u_{s,-h1}\frac{\partial h_1}{\partial x} = -\frac{\partial}{\partial x}[u_s(h_0 - h_1)] \tag{25}$$

Eq.(6) is integrated from $-h_1$ to z resulting in

$$0 = \frac{\partial}{\partial x}[u(z + h_1)] + w(z) - \left(w_{-h_1} + u_{-h_1}\frac{\partial h_1}{\partial x}\right)$$

From the interface continuity of mass flux and Eq.(25), the parenthesized term becomes

$$w_{-h_1} + u_{-h1}\frac{\partial h_1}{\partial x} = -\frac{\partial}{\partial x}[\epsilon u_s(h_0 - h_1)] \tag{26}$$

Finally, this gives

$$w(z) = -\frac{\partial}{\partial x}[u(z + h_1)] - \frac{\partial}{\partial x}[\epsilon u_s(h_o - h_1)] \tag{27}$$

Integration of Eq.(6) from $-h_1$ to η gives

$$0 = \frac{\partial}{\partial x}\int_{-h_1}^{\eta} u dz - \left(\frac{\partial \eta}{\partial x} u_\eta - w_\eta\right) - \left(\frac{\partial h_1}{\partial x} u_{-h_1} + w_{-h_1}\right)$$

Using the free surface kinematic boundary condition and Eq.(26) for the parenthesized terms, the last equation finally yields the continuity equation:

$$\frac{\partial \eta}{\partial t} = -\frac{\partial}{\partial x}[u(\eta + h_1)] - \frac{\partial}{\partial x}[\epsilon u_s(h_o - h_1)] \tag{28}$$

3.3 Second-order Approximation

To get a second-order formulation of the governing equations, the results of the first-order equations for the vertical velocities and pressures are utilized. Neglecting terms of $O(\varepsilon^3)$ and higher in the nondimensional equations and using the dimensional counterparts, the following results are obtained:

Equation (2):

$$\frac{\partial w}{\partial t} = -g - \frac{1}{\rho}\frac{\partial p}{\partial z}$$

Using Eq.(27), this becomes

$$-\frac{1}{\rho}\frac{\partial p}{\partial z} = g - \frac{\partial^2}{\partial t \partial x}[u(z+h_1)] - \frac{\partial^2}{\partial t \partial x}[(\epsilon u_s(h_o - h_1)] \tag{29}$$

Integrating Eq.(29) from z to η and applying the free surface dynamic boundary condition lead to

$$\frac{p(z)}{\rho} = g(\eta - z) - \frac{\partial^2}{\partial t \partial x}\left[u\frac{1}{2}\{(\eta + h_1)^2 - (z+h_1)^2\}\right] - \frac{\partial^2}{\partial t \partial x}[\epsilon u_s(h_o - h_1)(\eta - z)] \tag{30}$$

Equation (5):

$$C_r \frac{\partial w_s}{\partial t} = -g - \frac{1}{\rho}\frac{\partial p_s}{\partial z} - \frac{\epsilon\nu}{K_p} w_s$$

The left-hand side is evaluated using the first-order form of $w_s(z)$, Eq.(24), resulting in

$$-\frac{1}{\rho}\frac{\partial p_s}{\partial z} = g - \frac{\partial^2}{\partial t \partial x}[C_r u_s(z+h_o)] - \frac{\partial}{\partial x}\left[\frac{\epsilon\nu}{K_p} u_s(z+h_o)\right] \tag{31}$$

Integrating from z to $-h_1$ and invoking the interface continuity of pressure and Eq.(30), the last equation becomes

$$\frac{p_s(z)}{\rho} = g(\eta - z) - \frac{\partial^2}{\partial t \partial x}\left[\frac{u}{2}(\eta + h_1)^2\right] - \frac{\partial^2}{\partial t \partial x}[\epsilon u_s(h_o - h_1)(\eta + h_1)] -$$
$$-\frac{\partial^2}{\partial t \partial x}\left[C_r \frac{u_s}{2}\{(h_o - h_1)^2 - (h_o + z)^2\}\right] - \frac{\partial}{\partial x}\left[\frac{\epsilon\nu}{K_p}\frac{u_s}{2}\{(h_o - h_1)^2 - (h_o + z)^2\}\right] \tag{32}$$

Equations (30) and (32) highlight the effect of the vertical velocity on the pressure distribution. The last four terms in the last equation are due to the inclusion of the local vertical velocity in the second-order formulation and show that in oscillatory flows where this component is nontrivial, the distribution of pressure in both water layer and porous layer is not hydrostatic.

Next, in consonance with the vertical integration of the equations for the pressures, a depth-integrated horizontal velocity U is defined in the water layer such that

$$u(x,z,t) = U(x,t) + u^*(x,z,t) \tag{33}$$

where

$$U = \frac{1}{h_1 + \eta} \int_{-h_1}^{\eta} u dz \tag{34}$$

and u^* is the horizontal velocity deviation along the vertical and is $O(\varepsilon^2)$. The velocity u can then be expanded as a power series in the parameter ε,

$$u(x,z,t) = \varepsilon u_1(x,t) + \varepsilon^2 u_2(x,z,t) + \varepsilon^3 u_3(x,z,t) + \ldots \tag{35}$$

From Eq.(34),

$$U = \varepsilon \hat{u}_1 + \varepsilon^2 \hat{u}_2 + \varepsilon^3 \hat{u}_3 + \ldots \tag{36}$$

where

$$\hat{u}_1 = \frac{1}{h_1 + \eta} \int_{-h_1}^{\eta} u_1 dz \ldots$$

The terms following $\varepsilon \hat{u}_1$ in Eq.(36) are of $O(\varepsilon^3)$ and higher and may be dropped out giving

$$U \approx \varepsilon \hat{u}_1 \tag{37}$$

Returning to the governing equations with Eqs.(35) and (37), the terms on the left-hand side reduce to the following:

$$\frac{\partial u}{\partial t} = \frac{\partial U}{\partial t} + O(\varepsilon^3) + \ldots$$

$$u \frac{\partial u}{\partial x} = U \frac{\partial U}{\partial x} + O(\varepsilon^4) + \ldots$$

$$w \frac{\partial u}{\partial x} = O(\varepsilon^3) + \ldots$$

Substitution of these equations into Eq.(1), with the third-order and higher terms neglected, leads to the following:

$$\frac{\partial U}{\partial t} + U \frac{\partial U}{\partial x} = -\overline{\frac{1}{\rho} \frac{\partial p}{\partial x}} \tag{38}$$

where the overbar represents an averaging over the relevant depth. With the pressure p dependent on z and the left-hand side of Eq.(38) expressed in terms of depth-averaged values, Eq.(30) for the pressure $p(z)$ is differentiated with respect to x, depth-averaged evaluating all integrals, then substituted in the last equation. This finally gives the horizontal momentum equation in the water layer:

$$\frac{\partial U}{\partial t} + U \frac{\partial U}{\partial x} = -g \frac{\partial \eta}{\partial x} + \frac{\partial^3}{\partial t \partial x^2} \left[\frac{U}{3} (\eta + h_1)^2 \right] + \frac{\partial^3}{\partial t \partial x^2} \left[\frac{\epsilon U_s}{2} (h_o - h_1)(\eta + h_1) \right] \tag{39}$$

U_s in Eq.(39) defined as

$$U_s = \frac{1}{h_o - h_1} \int_{-h_o}^{-h_1} u_s dz \tag{40}$$

was obtained from a similar development for the porous layer. Parallel developments for the terms on the left-hand side of Eq.(4) using Eq.(40) give, to second order,

$$C_r\left(\frac{\partial U_s}{\partial t}+U_s\frac{\partial U_s}{\partial x}\right)=-\overline{\frac{1}{\rho}\frac{\partial p_s}{\partial x}}-\overline{\frac{\epsilon\nu}{K_p}u_s}-\overline{\frac{\epsilon^2 C_f}{\sqrt{K_p}}\sqrt{u_s^2+w_s^2}u_s} \tag{41}$$

Using Eq.(32) for $p_s(z)$, the right-hand side of Eq.(41) is evaluated, integrating all terms with overbars. This finally gives the horizontal momentum equation in the porous layer:

$$\begin{aligned}C_r\left(\frac{\partial U_s}{\partial t}+U_s\frac{\partial U_s}{\partial x}\right)=&-g\frac{\partial\eta}{\partial x}+\frac{\partial^3}{\partial t\partial x^2}\left[\frac{U}{2}(\eta+h_1)^2\right]+\\&+\frac{\partial^3}{\partial t\partial x^2}\left[\epsilon U_s(h_o-h_1)(\eta+h_1)\right]+\frac{\partial^3}{\partial t\partial x^2}\left[\frac{C_rU_s}{3}(h_o-h_1)^2\right]\\&-\frac{\partial^2}{\partial x^2}\left[\frac{\epsilon\nu}{K_p}\frac{U_s}{3}(h_o-h_1)^2\right]-\frac{\epsilon\nu}{K_p}U_s-\frac{\epsilon^2C_f}{\sqrt{K_p}}\sqrt{U_s^2+W_s^2}U_s\end{aligned} \tag{42}$$

The momentum equations (39) and (42) and the depth-integrated continuity equation (28), comprise a second-order formulation of the transformation of a surface disturbance in a depth-varying region with a porous layer, taking into account the effect of vertical acceleration, finiteness of the surface displacement and the momentum loss in the porous layer.

Under ordinary conditions, W_s in Eq.(42) is much less than U_s. By invoking the assumption that $H/h \ll 1$ and noting that the interface and impermeable boundaries are rigid and that the porous layer has a homogeneous makeup, the second-order formulation can be simplified to the following set of nonlinear equations:

$$\frac{\partial\eta}{\partial t}+\frac{\partial}{\partial x}[U(\eta+h_1)]+\frac{\partial}{\partial x}[\epsilon U_s h_p]=0 \tag{43}$$

$$\frac{\partial U}{\partial t}+U\frac{\partial U}{\partial x}+g\frac{\partial\eta}{\partial x}-\frac{h_1^2}{3}\frac{\partial^3U}{\partial t\partial x^2}-\frac{\epsilon h_p h_1}{2}\frac{\partial^3U_s}{\partial t\partial x^2}=0 \tag{44}$$

$$\begin{aligned}C_r\left(\frac{\partial U_s}{\partial t}+U_s\frac{\partial U_s}{\partial x}\right)&+g\frac{\partial\eta}{\partial x}-\frac{h_1^2}{2}\frac{\partial^3U}{\partial t\partial x^2}-\left(\frac{C_rh_p^2}{3}+\epsilon h_p h_1\right)\frac{\partial^3U_s}{\partial t\partial x^2}\\&-\frac{\epsilon\nu}{3K_p}\frac{\partial^2}{\partial x^2}[U_s h_p]+\frac{\epsilon\nu}{K_p}U_s+\frac{\epsilon^2C_f|U_s|}{\sqrt{K_p}}U_s=0\end{aligned} \tag{45}$$

These equations can be applied in determining the wave field for progressive and oscillatory waves. Although wave motion is usually characterized by periodicity, this property is not a prerequisite in applying the equations since the time dimension has been explicitly included. Hence, these equations can be applied to both regular and irregular waves with suitable boundary conditions.

The assumption of order $(h/l)^2$ in the nondimensionalized velocities precludes the application of the equations in deep water. In addition, consideration of the nonlinearity of the boundary conditions for the free surface conforms approximately to the region where finiteness of wave height is important. Therefore, the region of validity of the equation falls approximately where the cnoidal wave theory is valid. Lastly, the equations are applicable in a region where the only energy loss is through friction in the porous layer. When breaking is present, the additional energy dissipation must be considered.

4 Breaking Wave Transformation

Wave breaking usually occurs on the breakwater upslope resulting in dissipation of wave energy. The amount of energy dissipated by this phenomenon has been related to the mass flux rate across a vertical section beyond the breaking point. For a submerged permeable breakwater, considering that the mass flux is due to flow across both water and porous layers, the energy dissipated is accounted for by adding an energy dissipation term per unit mass, $f_D U$ in the water layer and $f_D \epsilon U_s$ in the porous layer, to the left-hand sides of Eqs.(44) and (45).

The dissipation function f_D (dimension: time^{-1}) for breaking on a sloping impermeable bed has been given by Watanabe and Dibajnia (1988). Recognizing the points of departure of the breaking dissipation over a submerged porous breakwater from that over an impermeable bed, the dissipation function was modified as

$$f_D = \alpha_D \tan\beta' \sqrt{\frac{g}{h_1'}} \sqrt{\frac{\varphi - \varphi_r}{\varphi_s - \varphi_r}} \tag{46}$$

where $\alpha_D = 2.5$, $\tan\beta'$ is the effective bottom slope at the breaking point, $h_1' = h_1 + \epsilon h_p$, $\varphi = |\bar{\eta}|/h_1'$, $\varphi_r = 0.4(|\bar{\eta}|/h_1')_b$, $\varphi_s = 0.5(0.57 + 5.3\tan\beta')$. The subscript b indicates values at the breaking point. $|\bar{\eta}|$ is the effective amplitude defined as $|\bar{\eta}| = 0.50(\eta_c - \eta_t)$ where η_c and η_t are the surface displacements of the crest and trough, respectively. A breaking criterion based on the experiments of Rojanakamthorn et. al. (1990) was used to locate the breaking point.

5 Application and Results

In applying Eqs.(43) to (45) within a region where structures are present, the waves reflected from the structure are subtracted through the offshore boundary by considering an appropriate boundary condition. For one dimension, this is expressed by

$$\eta(x_o, t + dt) = \eta_I(x_o, t + dt) + [\eta(x_o + C_o dt, t) - \eta_I(x_o + C_o dt, t)] \tag{47}$$

where C is the celerity, subscript I refers to a prescribed incident wave and o refers to the offshore location. At the onshore boundary, complete transmission

of the transformed wave is enforced through the radiation condition:

$$\left.\frac{\partial \eta}{\partial t}\right|_{x=x_D} = -C_D \left.\frac{\partial \eta}{\partial x}\right|_{x=x_D} \tag{48}$$

where the subscript D refers to the onshore location. The velocity U is similarly prescribed.

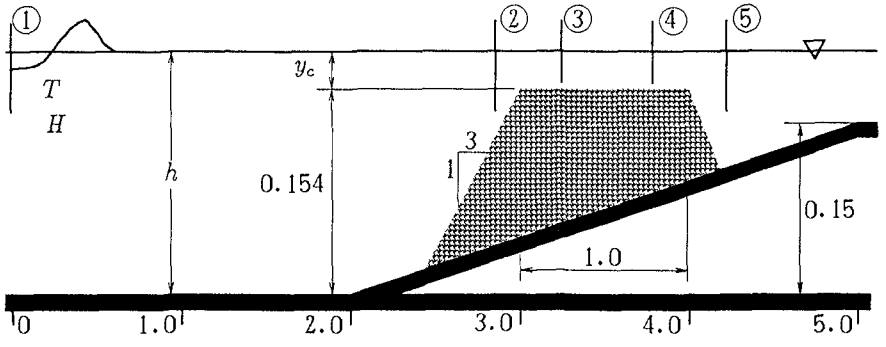

Figure 2: Submerged permeable breakwater

Equation (43) to (45) have been discretized for numerical computation using an eight-point finite-difference computational module on a staggered mesh. Calculation was carried out from still water conditions alternately for the velocities and η. The equations were tested for the case of monochromatic wave propagation on a horizontal bottom without any porous body by comparing with a theoretical solution for the spatial and temporal profiles of η. Calculation gives profiles that conform very well with those given by the second-order cnoidal wave theory.

Laboratory experiments were performed to examine the applicability of the nonlinear model to predicting wave transformation over a submerged permeable breakwater. The set-up is given in Fig. 2. One of the gauges was located beyond the structure to describe the disintegrated wave. In the calculations the properties of the fluid and porous material were: $\nu = 1.3 \times 10^{-6}\mathrm{m}^2/\mathrm{s}$, $\epsilon = 0.44$, $K_p = 2.06 \times 10^{-8}\mathrm{m}^2$, $C_f = 0.428$, $g = 9.8\mathrm{m}/\mathrm{s}^2$ and $C_r = 1.0$. The porosity was measured directly in the laboratory and K_p and C_f are fixed by the size of the gravel used.

Figures 3 and 4 show the comparison of the wave profiles at different locations when no breaking was observed anywhere in the wave flume. In Fig. 3, the relative depth of submergence H/y_c is 0.29 and the relative depth h/L offshore is 0.073. It can be seen that the weak disintegration at the breakwater lee is predicted by the second-order equations. Using the nonlinear incident wave based on the experiments for the offshore boundary condition leads to a large reflection

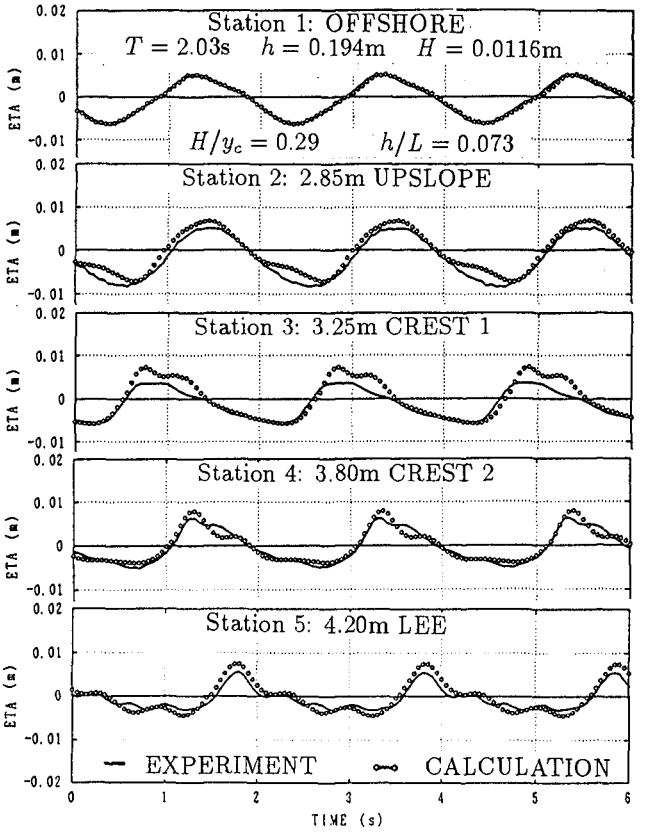

Figure 3: Wave Profiles (Case 1, Non-breaking transformation)

from the breakwater (Station 2) and a secondary peak at the first crest station. In Fig. 4, the water depth was reduced so that H/y_c becomes large, leading to a strong disintegration leeward. Although the high-frequency components of the disintegrated wave are not reproduced, the general pattern is predicted by the second-order equations.

For breaking transformation, the dissipation function is evaluated at all points beyond the breaking point using Eq.(46). Figure 5 shows a comparison of the wave profiles from calculation and experiments for a short period incident wave. The breaking point was located at $x = 2.95$m in both calculation and experiment. For this case, the wave height was increased so that $H/y_c = 0.99$ and $h/L = 0.136$. It is evident that the model predicts the wave height distribution well. However, the second-order equations fail to yield the secondary component of the transmitted wave at the lee.

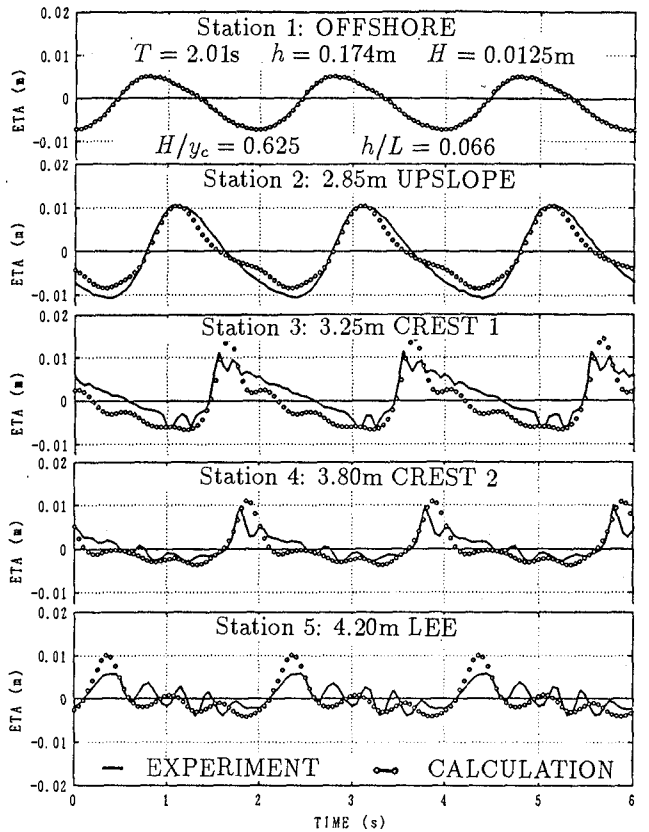

Figure 4: Wave Profiles (Case 2, Non-breaking transformation)

6 Conclusions

1. Basic equations of nonlinear wave transformation over a porous layer are derived.

2. For non-breaking transformation on the submerged permeable breakwater, the equations predict the wave height and the profile well. However, the disintegrating characteristic of the transmitted waves is weakly predicted by the second-order equations.

   When H_i/y_c is less than about 0.29, the agreement is good while for higher ratios, the agreement is not good especially at the breakwater lee.

3. For breaking transformation, the wave profiles are predicted well prior to the region leeward of the breakwater where the waves disintegrate. Although the wave profile is not reproduced so well after breaking, the wave height distribution is predicted fairly well by the present model of wave breaking.

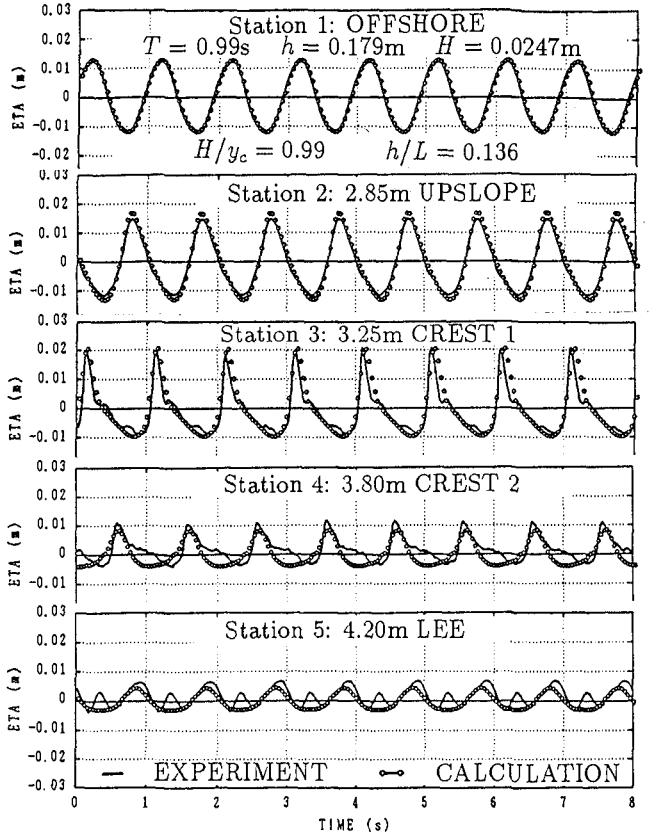

Figure 5: Wave Profiles (Breaking transformation)

References

1. Rojanakamthorn, S., M. Isobe and A. Watanabe (1990): Modeling of wave transformation on submerged breakwater, Proceedings, 22nd Coastal Engineering Conference, ASCE, 1060-1073

2. Shuto, N. and S. Hashimoto (1970): Hydraulic resistance of artificial concrete blocks, Proceedings, 12th Coastal Engineering Conference, ASCE, 43-54

3. Watanabe, A. and M. Dibajnia (1988): A numerical model of wave deformation in the surf zone, Proceedings, 21st Coastal Engineering Conference, ASCE, 578-587